Characterization of a Grapevine R2R3-MYB Transcription Factor That Regulates the Phenylpropanoid Pathway[1][W]

Laurent Deluc[2], François Barrieu, Chloé Marchive, Virginie Lauvergeat, Alain Decendit, Tristan Richard, Jean-Pierre Carde, Jean-Michel Mérillon, and Saïd Hamdi*

Unité Mixte de Recherche 619, Physiologie et Biotechnologie Végétales, Université Bordeaux 1, Université Bordeaux 2, Institut National de la Recherche Agonomique, Centre de Recherche de Bordeaux, 33883 Villenave d'Ornon, France (L.D., F.B., C.M., V.L., J.-P.C., S.H.); and Laboratoire de Mycologie et de Biotechnologie Végétale EA3675, Université Bordeaux 2, 33076 Bordeaux cedex, France (A.D., T.R., J.-M.M.)

The ripening of grape (*Vitis vinifera*) berry is characterized by dramatic changes in gene expression, enzymatic activities, and metabolism that lead to the production of compounds essential for berry quality. The phenylpropanoid metabolic pathway is one of the components involved in these changes. In this study, we describe the cloning and functional characterization of *VvMYB5a*, a cDNA isolated from a grape L. cv Cabernet Sauvignon berry library. *VvMYB5a* encodes a protein belonging to a small subfamily of R2R3-MYB transcription factors. Expression studies in grapevine indicate that the *VvMYB5a* gene is mainly expressed during the early steps of berry development in skin, flesh, and seeds. Overexpression of *VvMYB5a* in tobacco (*Nicotiana tabacum*) affects the expression of structural genes controlling the synthesis of phenylpropanoid and impacts on the metabolism of anthocyanins, flavonols, tannins, and lignins. Overexpressing *VvMYB5a* induces a strong accumulation of several phenolic compounds, including keracyanin (cyanidin-3-rhamnoglucoside) and quercetin-3-rhamnoglucoside, which are the main anthocyanin and flavonol compounds in tobacco. In addition, *VvMYB5a* overexpression increases the biosynthesis of condensed tannins and alters lignin metabolism. These findings suggest that *VvMYB5a* may be involved in the control of different branches of the phenylpropanoid pathway in grapevine.

Phenylpropanoids are a diverse group of plant secondary metabolites, including anthocyanins, flavonols, proanthocyanidins (PAs), and lignins (Fig. 1), that accumulate in a wide variety of plant tissues. In grape (*Vitis vinifera*) berry, flavonoids, like flavonols, protect the plant against UV radiations (Winkel-Shirley, 2002), whereas others, such as anthocyanins, help attract seed-dispersal agents. Moreover, PAs subsequently lead to condensed tannins (CTs), which are known to protect plants against microbial and fungal growth (Dixon et al., 2005).

Flavonoids also play an important role in the quality of wine. Anthocyanin compounds are the major constituents of red wine color. CTs are important organoleptic components of wines because they are responsible for bitterness and astringency. They are also considered critical elements in the stability of red wine color (Glories, 1988). In addition to these properties, nutrient and health benefits have been reported for nearly all classes of phenylpropanoids, especially stilbenes such as trans-resveratrol (Pervaiz, 2003). Flavonoids, which increase the antioxidant capacity of cells and tissues (Hollman and Katan, 1999; Lairon and Amiot, 1999; Bagchi et al., 2000), are responsible for the antioxidant property of red wine. In vitro studies have revealed the powerful antioxidant properties of some anthocyanins from grape berry such as malvidin 3-*O*-β-glucoside and peonidin 3-*O*-β-glucoside (Fauconneau et al., 1997; Mérillon et al., 1997). PAs are also powerful antioxidants with beneficial effects on human cardiac health (Bagchi et al., 2003) and immunity (Lin et al., 2002). As a consequence, moderate red wine drinkers have a reduced risk of cardiovascular disease and cancer (Klatsky, 2002).

Even though the polyphenol composition of grape berries has been extensively studied (Boss et al., 1996; Kennedy et al., 2000; Downey et al., 2003), little is known about the regulation of genes involved in the flavonoid pathway during berry development. In plants, regulation of the genes involved in flavonoid metabolism has been studied in petunia (*Petunia hybrida*), maize (*Zea mays*), snapdragon (*Antirrhinum majus*), and Arabidopsis (*Arabidopsis thaliana*; Cone et al., 1986; Paz-Ares et al., 1987; Martin et al., 1991; Quattrochio et al., 1993; Holton and Cornish, 1995; Mol et al., 1998; Borevitz et al., 2000) and more recently in fruit

[1] This work was supported by grants from the Conseil Interprofessionnel du Vin de Bordeaux.

[2] Present address: Department of Biochemistry, University of Nevada, Reno, NV 89557.

* Corresponding author; e-mail said.hamdi@bordeaux.inra.fr; fax 33–5–57–12–25–41.

The author responsible for distribution of materials integral to the findings presented in this article in accordance with the policy described in the Instructions for Authors (www.plantphysiol.org) is: Saïd Hamdi (said.hamdi@bordeaux.inra.fr).

[W] The online version of this article contains Web-only data.

Article, publication date, and citation information can be found at www.plantphysiol.org/cgi/doi/10.1104/pp.105.067231.

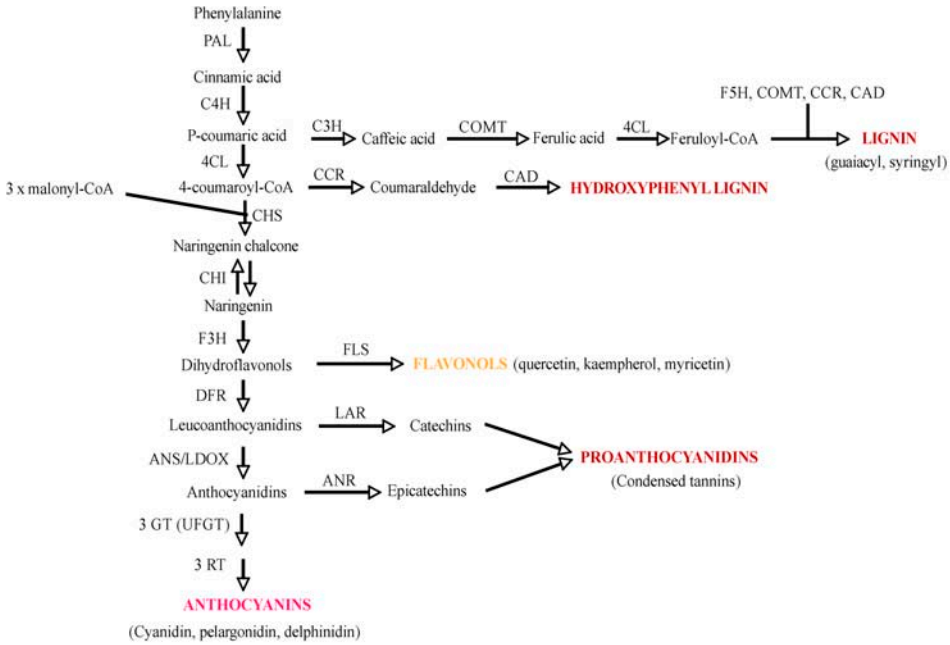

Figure 1. Scheme of branch pathways of phenylpropanoid metabolism in plants leading to the synthesis of anthocyanins, flavonols, PAs, and lignin. Enzymes that function in multiple or specific pathways are indicated. Abbreviations are as follows: ANR, anthocyanidin reductase; ANS/LDOX, anthocyanidin synthase; CAD, cinnamyl alcohol dehydrogenase; C4H, cinnamate 4-hydroxylase; CCR, cinnamyl-CoA reductase; C3H, 4-coumarate 3-hydroxylase; 4CL, 4-coumarate-CoA ligase; CHS, chalcone synthase; CHI, chalcone isomerase; COMT, caffeic acid *O*-methyltransferase; DFR, dihydroflavonol 4-reductase; F3H, flavanone 3-hydroxylase; F3′H, flavonoid 3′-hydroxylase; F5H, ferulate 5-hydroxylase; FLS, flavonol synthase; 3GT (UFGT), UDPG-flavonoid-3-*O*-glucosyltransferase; LAR, leucoanthocyanidin reductase; LDOX, leucoanthocyanidin dioxygenase; PAL, Phe ammonia-lyase; 3RT, anthocyanidin-3-glucoside rhamnosyl transferase.

species (Aharoni et al., 2001; Mathews et al., 2003). These studies have identified a conserved regulatory mechanism of the flavonoid biosynthetic pathway, which appears to be under the control of two families of transcription factors, the MYC and MYB proteins. In grape berry, the coordinated expression of most of the structural genes involved in this pathway, except UDP Glc:flavonoid-3-*O*-glucosyltransferase (UFGT), suggests the involvement of two groups of regulatory factors during berry ripening (Boss et al., 1996). The first group might control expression of Phe ammonia-lyase (PAL), chalcone synthase (CHS), chalcone isomerase (CHI), flavanone 3-hydoxylase (F3H), dihydroflavonol 4-reductase (DFR), and anthocyanidin synthase (ANS), and the other induces UFGT gene expression. If this were so, the first regulatory genes would have to be expressed early in berry development, whereas a second group of transcription factors triggering among others UFGT expression would be expressed when grape ripening begins (e.g. after véraison). Recently, a *MYB*-related gene associated with the regulation of the *UFGT* gene was identified in *Vitis labruscana* berries (Kobayashi et al., 2002). Retrotransposon-induced mutations in this gene, named *VvMYBA1*, are associated with the lack of anthocyanin biosynthesis in white cultivars of Vitis (Kobayashi et al., 2004). To date, no study, to our knowledge, has isolated the *MYB* regulatory genes expressed in the early stages of berry development and potentially involved in the regulation of flavonoid gene expression. In this study, we report the functional characterization of a transcriptional regulator, named *Vv*MYB5a, isolated from a Cabernet Sauvignon cDNA library. The *VvMYB5a* gene belongs to a small cluster of *R2R3-MYB* genes and is mainly expressed in the early steps of berry development. Overexpression of *VvMYB5a* in tobacco (*Nicotiana tabacum*) affects the expression levels of flavonoid structural genes and leads to high accumulation of anthocyanins and PAs, especially in flowers. In addition, *Vv*MYB5a is also involved in the regulation of monolignol metabolism, thus delaying anther development. Taken together, our findings indicate that *Vv*MYB5a might represent a R2R3-MYB transcription factor potentially involved in the control of various parts of the phenylpropanoid pathway in plants.

RESULTS

*Vv*MYB5a Sequence Features

Using PCR on a grape berry cDNA library at the véraison stage, we identified one clone, named *VvMYB5a*, encoding a putative R2R3 MYB protein. *VvMYB5a* appeared to be a full-length cDNA of 1,213 bp encoding a protein of 320 amino acids. The amino-terminal extremity contains the R2R3 imperfect repeats

responsible for binding to target DNA sequences and is highly conserved among R2R3-MYB proteins (Fig. 2A; Solano et al., 1995). The DNA-binding domain also contains a shorter sequence closely related to amino acid residues found in the maize transcriptional activator C1 (Grotewold et al., 2000) and required to interact with a basic helix-loop-helix cofactor (IR domain; Fig. 2A). In addition to the conserved C1 motif (Kranz et al., 1998), two other motifs were detected in the *Vv*MYB5a protein (Fig. 2A). The first motif, named C3, is found only in a few MYB proteins with no clear physiological function (Li et al., 1996). The second motif is a Gln-rich domain (Fig. 2A), QQQQQQQQLQQV-QQP, with no assigned biological function at this time. Finally, no C2 motif (Jin et al., 2000) was found on the *Vv*MYB5a protein.

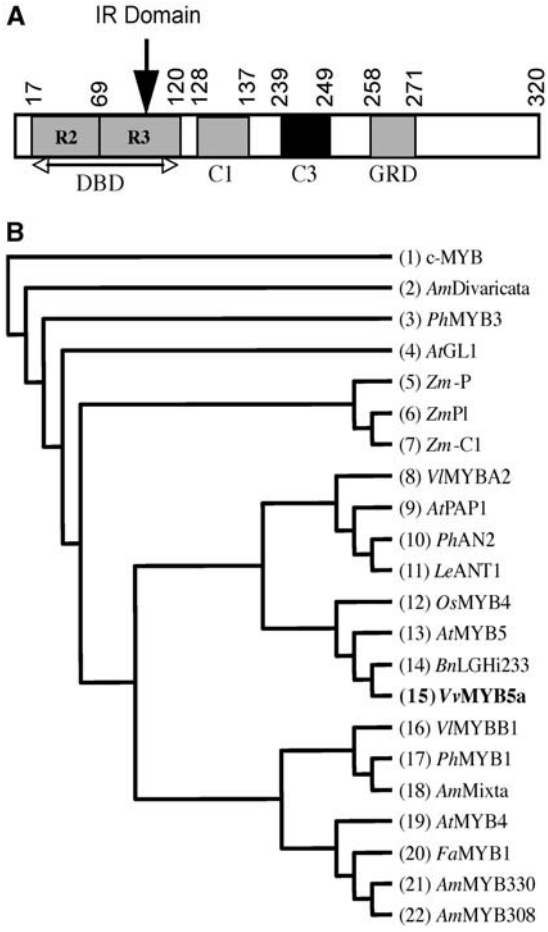

Figure 2. Features of *Vv*MYB5a protein. A, Schematic representation of the major functional domains in the *Vv*MYB5a protein based on data derived from sequence comparisons. R2 and R3 are the two repeats of the MYB DNA-binding domain (DBD). The IR domain corresponds to the residues involved in putative interaction with MYC proteins (glutamine-rich domain [GRD]). B, Phylogenetic analysis of a selection of plant MYB proteins was performed by using a BLAST algorithm on the GenBank and EMBL databases. The *Vv*MYB5a protein sequence was aligned to known plant MYB sequences, and their distance relationships were resolved using the neighbor-joining tree-building method. The human protein c-MYB is used as an outgroup. See "Materials and Methods" for accession numbers.

A phylogenetic analysis of 22 plant MYB proteins by the neighbor-joining method (Fig. 2B) indicates that *Vv*MYB5a belongs to a distinct cluster of four MYB proteins with no assigned biological functions at this time. This small cluster does not contain any other MYB proteins from Vitis such as *Vl*MYBA and B (Kobayashi et al., 2002). Regarding the sequence homology, the overall *Vv*MYB5a protein sequence shares little homology with known MYB proteins. The nearest neighbor, a cotton (*Gossypium hirsutum*) seed MYB factor, named *Bn*GHl233, displays only 59% overall identity with the *Vv*MYB5a protein sequence.

VvMYB5a Expression in Grapevine Tissues

VvMYB5a expression in both vegetative and reproductive grapevine plant tissues was analyzed by semiquantitative reverse transcription (RT)-PCR followed by Southern blotting using the *VvMYB5a* 3′-untranslated region (UTR) as a radiolabeled probe to avoid cross hybridization with other members of the MYB gene family (Fig. 3). Expression was detected in all tissues studied with the highest levels in berries and leaves. In berry (Fig. 3A), *VvMYB5a* expression appeared high in the early stages of development and then decreased rapidly to a very low level after the véraison stage 8 weeks after flowering. The same pattern was observed in flesh, skin, and seed tissues with a high expression in skin 6 weeks after flowering compared to other berry tissues (Fig. 3B). In leaves, *VvMYB5a* expression was high compared to root tissues and was not modified by the developmental stages (Fig. 3C). In summary, expression of the *VvMYB5a* gene is not fruit specific but is clearly down-regulated during grape berry development and in a similar way in different fruit tissues.

Overexpression of *VvMYB5a* in Tobacco May Affect the Expression of General Phenylpropanoid Biosynthetic Genes

To ascertain a putative function for *VvMYB5a*, we used tobacco as a model system for heterologous expression experiments. Primary transformants, T_1 and T_2 generation of transgenic tobacco plants overexpressing *VvMYB5a* under the control of the cauliflower mosaic virus 35S promoter, showed no significant differences in growth compared to wild-type lines. Because several MYB proteins are known to play important roles in transcriptional regulation of phenylpropanoid biosynthetic genes, the effect of *VvMYB5a* overexpression on three genes encoding enzymes related to the general phenylpropanoid metabolism (Fig. 1) was examined by semiquantitative RT-PCR analyses in leaves of transgenic plants (Fig. 4, A and B). Expression of PAL and 4-coumaroyl-CoA ligase (4CL) appeared unaffected by *VvMYB5a* overexpression. In contrast, expression of the gene encoding cinnamate 4-hydroxylase (C4H) was slightly, but significantly, induced in leaves of transgenic lines compared to wild-type nontransformed plants (Fig. 4B).

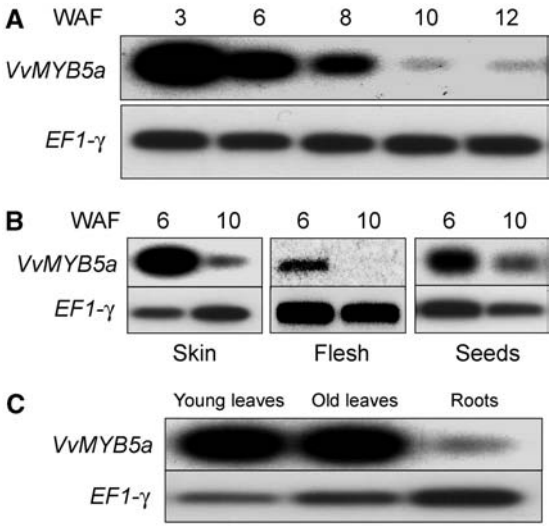

Figure 3. *VvMYB5a* expression in grapevine tissues. Southern blots of semiquantitative RT-PCR products blotted onto nylon membrane and hybridized with the radiolabeled *VvMYB5a* 3′-UTR probe. Elongation factor *EF1-γ* was used as a control. A, Expression of *VvMYB5a* during grape berry development (berry flesh and skin). B, Expression of *VvMYB5a* in berry tissues. C, Expression of *VvMYB5a* in grapevine tissues harvested from fruit cutting.

Accumulation of Anthocyanin and PA-Derived Compounds in Transgenic Tobacco Flowers

If the vegetative parts of the *VvMYB5a*-overexpressing plants were not showing any phenotypic differences when compared to wild-type plants, significant changes in coloring were detected in petals of transgenic tobacco flowers (Fig. 5, B and F). The most important modifications were observed in stamens, where the amount of pigmentation was clearly greater in transgenic stamens (Fig. 5, D and H) than in control stamens (Fig. 5, C and G). Another aspect that appeared in transgenic lines was the accumulation of CTs in transgenic petals. Dimethylaminocinnamaldehyde (DMACA) reagent, known to interact with CTs (Xie et al., 2003), provided a blue staining in epidermal cells of petal limbs from *Vv*MYB5a lines that was not observed in the control plants (Fig. 5, I and J). HPLC analysis and quantification indicate a significant accumulation of epicatechin-derived compounds together with a high concentration of free monomer units of CT (10.2 ± 0.08 mg/g fresh weight) in transgenic petals compared to wild-type plants (1.18 ± 0.43 mg/g fresh weight; Table I). CT accumulation was also detected in transgenic seeds with increased levels in the seed coat compared to control seeds (Fig. 5, K and L). No CT accumulation was observed in stamens regardless of the developmental stage.

Quantification and Identification of Anthocyanins from Petal and Stamen Extracts

Chromatographic profiles at 521 nm (Fig. 6) identified anthocyanin compounds and other flavonoids and provided interesting results with regard to the differential distribution of polyphenolic compounds in petal limbs and stamens from transgenic or control plants. In control plants, all compounds present in petal limbs were detected in small quantities in stamen tissues (peaks 2, 4, and 5) or were absent, as shown by peaks 1 and 3 (Fig. 6, A and B).

In petal limbs of transgenic tobacco, overexpression of *VvMYB5a* triggered a slight increase in most compounds cited above with the exception of compound 2,

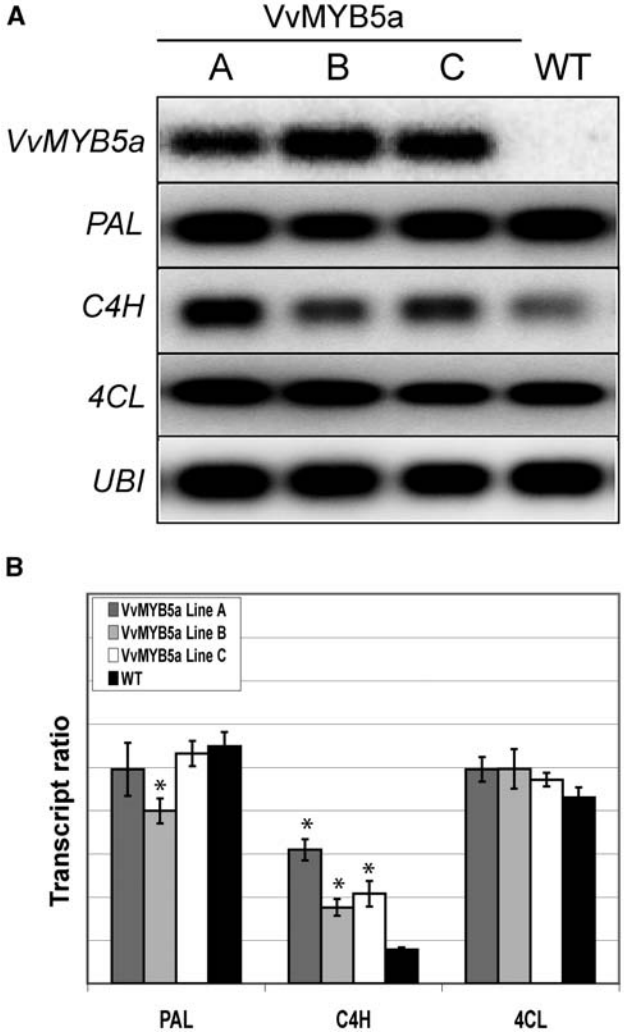

Figure 4. Analysis of general phenylpropanoid gene expression in leaves of transgenic tobacco overexpressing *Vv*MYB5a. A, Transcripts for three biosynthetic genes of the general phenylpropanoid metabolism (*PAL*, *C4H*, and *4CL*) were detected by semiquantitative RT-PCR in leaves from three *VvMYB5a* independent lines (A–C) and compared to wild-type lines. *VvMYB5a* indicates the transgene expression level. *UBI* was used as a quantitative control. B, Quantification of the RT-PCR results shown in A was performed by measuring the intensity per millimeters squared (Quantity One software; Bio-Rad) of the bands and calculating the ratios between the bands in the gene-specific blot and its corresponding band in the UBI control blot (transcript ratio). Data are means ± SE of two semiquantitative RT-PCR experiments from two independent RNA extractions. Asterisk (*) indicates a significant difference from wild-type plants ($P \leq 0.01$; Student's *t* test).

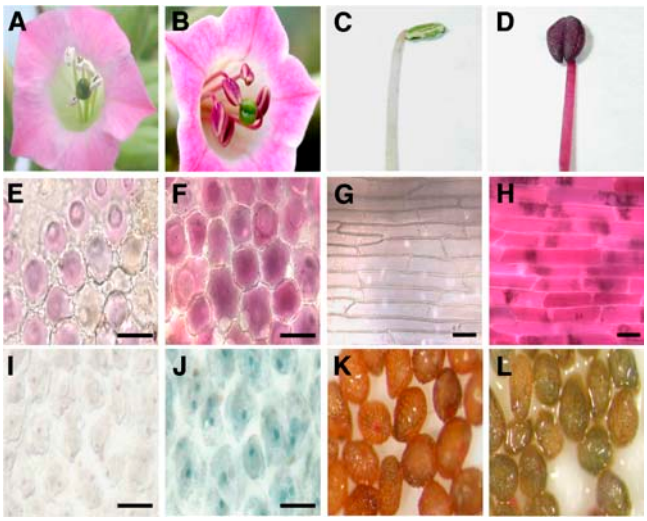

Figure 5. Accumulation of phenylpropanoid compounds in *VvMYB5a*-overexpressing plants. Flowers of transgenic plants (B) showed a clear phenotypic change in petal and stamen pigmentation compared to wild-type flowers (A). Increased pigmentation is observed in petal epidermal cells of transgenic plants (F) compared to control lines (E). A strong red pigmentation is also observed in transgenic stamen epidermal cells (D and H) compared to wild-type stamens (C and G). DMACA staining of petal cells (J) and seed coats (L) from transgenic lines show CT accumulation compared to control petals (I) and seeds (K). E to J, Bars = 50 μm.

which surprisingly decreased compared to the wild-type sample (Fig. 6A). On the other hand, a spectacular increase in peak 3 (retention time = 17 min) was observed in stamens, together with a weak increase in peaks 4 and 5 and the appearance of peak 1 (Fig. 6B). Peak 3 was collected and found to yield a pure compound. Fast-atom bombardment$^+$ mass spectroscopy showed $[M]^+$ peak at mass-to-charge ratio = 595 consistent with molecular formula $C_{27}H_{31}O_{15}$. The structure of this compound was elucidated by ^{1}H- and ^{13}C-NMR experiments (see Supplemental Table I). By comparison with the literature (Torskangerpoll et al., 1999) and our experimental data, the aglycon was confirmed to be cyanidin with a Rha and a Glc unit. The compound was finally identified as cyanidin 3-*O*-(6″-*O*-α-rhamnopyranosyl-β-glucopyranoside), also known as keracyanin. Cochromatography with an authentic standard confirmed this identification. Quantitative determination of total anthocyanin content was performed by spectrophotometry in stamens and petal limbs (Table II). The largest variations were detected for stamen tissue, with a total estimated anthocyanin concentration of 4.33 ± 0.08 mg/g dry weight for transgenic plants, whereas no basal level was detected in wild-type plants. In transgenic petal limbs, a slight, but significant, accumulation was present (3.39 ± 0.09 mg/g dry weight) as compared to wild type (1.48 ± 0.26 mg/g dry weight). HPLC quantification of cyanidin-3-rhamnoglucoside content confirmed the increase in anthocyanin production in transgenic petals and stamens (Table III). The anthocyanin metabolic pathway in the various tissues studied gave an unequal production of cyanidin-3-rhamnoglucoside because it represented 83% of total anthocyanin content in *VvMYB5a* stamens, 61% in *VvMYB5a* petals, and 80% in wild-type petals. In addition to these analyses regarding anthocyanin-derived compounds, peak 5, which increases slightly in transgenic petals and stamens (Fig. 6, A and B), yielded a pure compound that was identified as rutin (quercetin 3-*O*-(6″-*O*-α-rhamnopyranosyl-β-glucopyranoside) by mass spectrometry and ^{1}H- and ^{13}C-NMR (see Supplemental Table II). In summary, *VvMYB5a* overexpression enhances the anthocyanin biosynthetic pathway, but several lines of evidence suggest that the production of other flavonoid compounds is altered in transgenic lines.

VvMYB5a-Regulated Phenylpropanoid Gene Expression in Flowers

RT-PCR analysis (Fig. 7, A–D) for three independent lines indicated that *Vv*MYB5a can act as an activator of expression of different phenylpropanoid structural genes in tobacco flowers. In stamens (Fig. 7, C and D), expression of genes involved in the flavonoid biosynthetic pathway, like CHS, CHI, F3H, and DFR, appeared strongly up-regulated compared to wild-type plants. A moderate increase in expression of CHS, CHI, and F3H was also detected in petal limbs of two out of three transgenic lines. In addition, the expression of DFR in petals was clearly down-regulated compared to wild-type plants (Fig. 7, A and B). Northern-blot analysis using a heterologous ANS cDNA probe from Petunia revealed an enhancement in transcript levels in transgenic petal limbs but no up-regulation was detected in stamens (Fig. 7E). Taken together, these results indicate that the regulatory mechanisms of gene expression by *Vv*MYB5a could be different between these two organs.

Disruption of Anther Development and Modification of Lignin Metabolism in *VvMYB5a*-Overexpressing Plants

Anther development was monitored in plants overexpressing *VvMYB5a* and in wild type. The overall development was similar in both lines with regard to

Table I. *Epicatechin and catechin content (milligrams per gram fresh weight tissue) of wild-type and transgenic plants from petal extracts*

Quantitative determination of catechin and epicatechin content in tobacco flowers has been performed by HPLC. The eluate was monitored at 280 nm. Purified standards of catechin and epicatechin were used as controls. Data are the means ± SD of two replicates. N.D., Not detected.

Sample	Catechin	Epicatechin
VvMYB5a line A	N.D.	10.05 ± 0.56[a]
VvMYB5a line B	N.D.	11.22 ± 0.47[a]
VvMYB5a line C	N.D.	9.35 ± 0.64[a]
Wild-type plants	N.D.	1.18 ± 0.43

[a]Significantly different from wild type ($P < 0.005$; Student's *t* test).

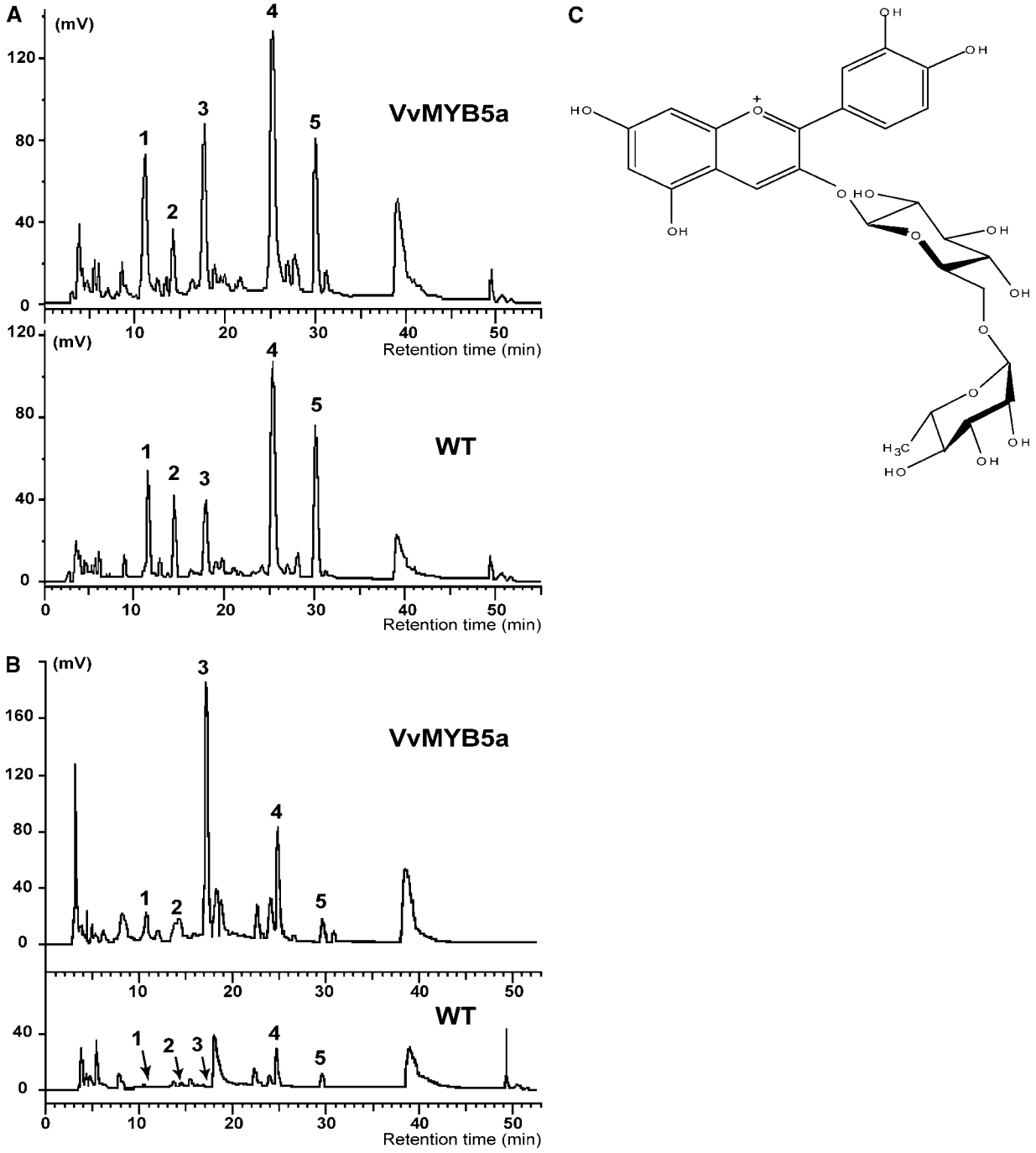

Figure 6. HPLC analysis of methanolic extracts from control and *VvMYB5a* petals and stamens. A, HPLC chromatograms at 521 nm from transgenic (*VvMYB5a*) and control (wild-type) petals. B, HPLC chromatograms at 521 nm from transgenic (*VvMYB5a*) and control (wild-type) stamens. Peaks 1, 2, and 4 are unknown. Peak 3 corresponds to cyanidin-3-rhamnoglucoside and peak 5 corresponds to quercitin-3-rhamnoglucoside. Each chromatogram has been obtained from the same injected quantity of sample (0.375 mg dry weight).

size and shape of the anthers and filaments. However, anthers of the transgenic line remained undehiscent, whereas pollen grains were freely released from wild-type flowers at the same stage. Germination experiments showed that male sterility of transformed plants was not related to the production of abnormal pollen (data not shown).

Cross sections of tobacco inflorescences before dehiscence showed that anther development was not affected in transgenic plants during the early stages of development described by Koltunow et al. (1990; data not shown). However, while dehiscence occurred in wild-type lines, the anthers stayed closed in the transgenic ones. Close inspection of the anther endothecium

Table II. *Total anthocyanin content (milligrams per gram dry weight tissue) of wild-type and transgenic plants from stamen and petal extract*

Quantitative determination of total anthocyanin content in tobacco flowers has been performed by spectrophotometry at 535 nm. A purified standard of keracyanin was used as a control. Data are the means ± SD of four replicates. N.D., Not detected.

Sample	Stamens	Petals
VvMYB5a line A	4.93 ± 0.07	3.51 ± 0.12[a]
VvMYB5a line B	4.20 ± 0.09	3.42 ± 0.07[a]
VvMYB5a line C	3.86 ± 0.08	3.24 ± 0.08[a]
Wild-type control	N.D.	1.48 ± 0.26

[a]Significantly different from wild type ($P < 0.001$; Student's *t* test).

showed that this difference was likely related to changes occurring during lignification of the endothecial cell wall (Fig. 8A). During maturation of the endothecial cells, from stage 4 to stage 10, secondary lignified thickenings (fibrous bands) grew along the radial walls of the endothecium but not on the tangential ones (Fig. 8A, II and V). This rigid frame allowed shrinkage of the endothecial cells, breaking of stomium, and release of pollen grains. In transformed plants, fewer endothecial cells developed lignified fibers and these fibers were more often incomplete, covering only part of the radial walls (Fig. 8A, III and VI). In these conditions, the rigidity of the wall frame was lower and the subsequent shrinkage of the anther walls resulting in the release of pollen grains in wild-type plants did not occur in transgenic ones.

Expression studies of structural genes involved in the monolignol biosynthetic pathway such as cinnamyl alcohol dehydrogenase (*CAD*), caffeic acid-*O*-methyltransferase (*COMT*) *I*, and caffeoyl coenzyme A 3-*O*-methyltransferase (*CCoAOMT*) *1*, *5*, and *6* were performed in tobacco anther tissues (Fig. 8B). If transcript levels of *CAD*, *COMT I*, and *CCoAOMT5* remain unaffected by *VvMYB5a* overexpression, a clear decrease of *CCoAOMT1* gene expression was observed in transgenic lines. Expression level of *CCoAOMT6* also appeared lower in stamens of two out of three transgenic lines when compared to wild type (Fig. 8C).

DISCUSSION

*Vv*MYB5a, a Particular Type of R2R3-MYB Protein?

This study shows that constitutive overexpression of *VvMYB5a*, a cDNA encoding a R2R3-MYB transcription factor from grape berry, results in clear phenotypic changes in tobacco. The whole phenylpropanoid pathway was affected with a general increase in the levels of flavonols, anthocyanins, PAs, and a decrease in monolignols. Except for *AtPAP1*, which triggers the activation of the lignin and anthocyanin pathways in Arabidopsis (Borevitz et al., 2000), it is unusual that a single gene is able to control different branches of the same metabolic pathway. Global and local protein analyses showed weak sequence homology between *Vv*MYB5a and other known R2R3-MYB proteins whose functions have already been investigated, including *At*PAP1. Analyses restricted to the usually well-conserved R2R3 domain indicate that the closest homolog for the *Vv*MYB5a R2R3 domain is found on the repressor *At*MYB4, with only 66% sequence homology, followed by 64% of homology for *Am*MYB330 and *Am*MYB308 domains. However, these MYB factors are all involved in the repression of target gene expression and contain the conserved C2 motif $pdLNL^{D}/_{E}lxi^{G}/_{S}$ in their C-terminal region that was not detected in *Vv*MYB5a (Jin et al., 2000; Aharoni et al., 2001). Without ruling out the possibility of a repressive action mode for *Vv*MYB5a, the absence of a C2 motif suggests that it might act differentially in the control of phenylpropanoid biosynthetic gene expression. Another interesting element within the protein sequence of *Vv*MYB5a is the presence of a conserved motif, named C3, which is found exclusively in the three nearest homologs of *Vv*MYB5a: *At*MYB5, *Bn*GHi233, and *Os*MYB4. Although *Os*MYB4 appears to be involved in plant chilling tolerance (Vannini et al., 2004), the functionality of *At*MYB5 and *Bn*GHi233 is not well understood; however, none of these regulatory proteins appear to be involved in the control of the flavonoid pathway (Li et al., 1996). According to Kranz and Stracke classifications (Kranz et al., 1998; Stracke et al., 2001), where in Arabidopsis *At*MYB5 belongs to a subgroup represented only by itself, the sequence homology between *Vv*MYB5a, *At*MYB5, *Bn*GHi233, and *Os*MYB4 might indicate the emergence of a small MYB cluster with members like *Os*MYB4 and *Vv*MYB5a involved in the control of surprisingly various physiological functions.

Overexpression of *VvMYB5a* Impacts on Different Branches of the Phenylpropanoid Pathway

The results presented in this study indicate that a single *R2R3-MYB* gene, *VvMYB5a*, may impact not only on one or two branches of the phenylpropanoid pathway, but on nearly the whole pathway when overexpressed in tobacco. Thus, overexpression of *VvMYB5a* affects the expression of various phenylpropanoid

Table III. *Keracyanin content (milligrams per gram dry weight tissue) of wild-type and transgenic plants from stamen and petal extract*

Quantitative determination of keracyanin content in tobacco flowers has been performed by HPLC. The eluate was monitored at 521 nm. A purified standard of keracyanin was used as a control. Data are the means ± SD of four replicates. N.D., Not detected.

Sample	Stamens	Petals
VvMYB5a line A	3.81 ± 0.41	2.20 ± 0.05[a]
VvMYB5a line B	3.54 ± 0.39	2.02 ± 0.04[a]
VvMYB5a line C	3.42 ± 0.31	1.99 ± 0.12[a]
Wild-type plants	N.D.	1.18 ± 0.42

[a]Significantly different from wild type ($P < 0.01$; Student's *t* test).

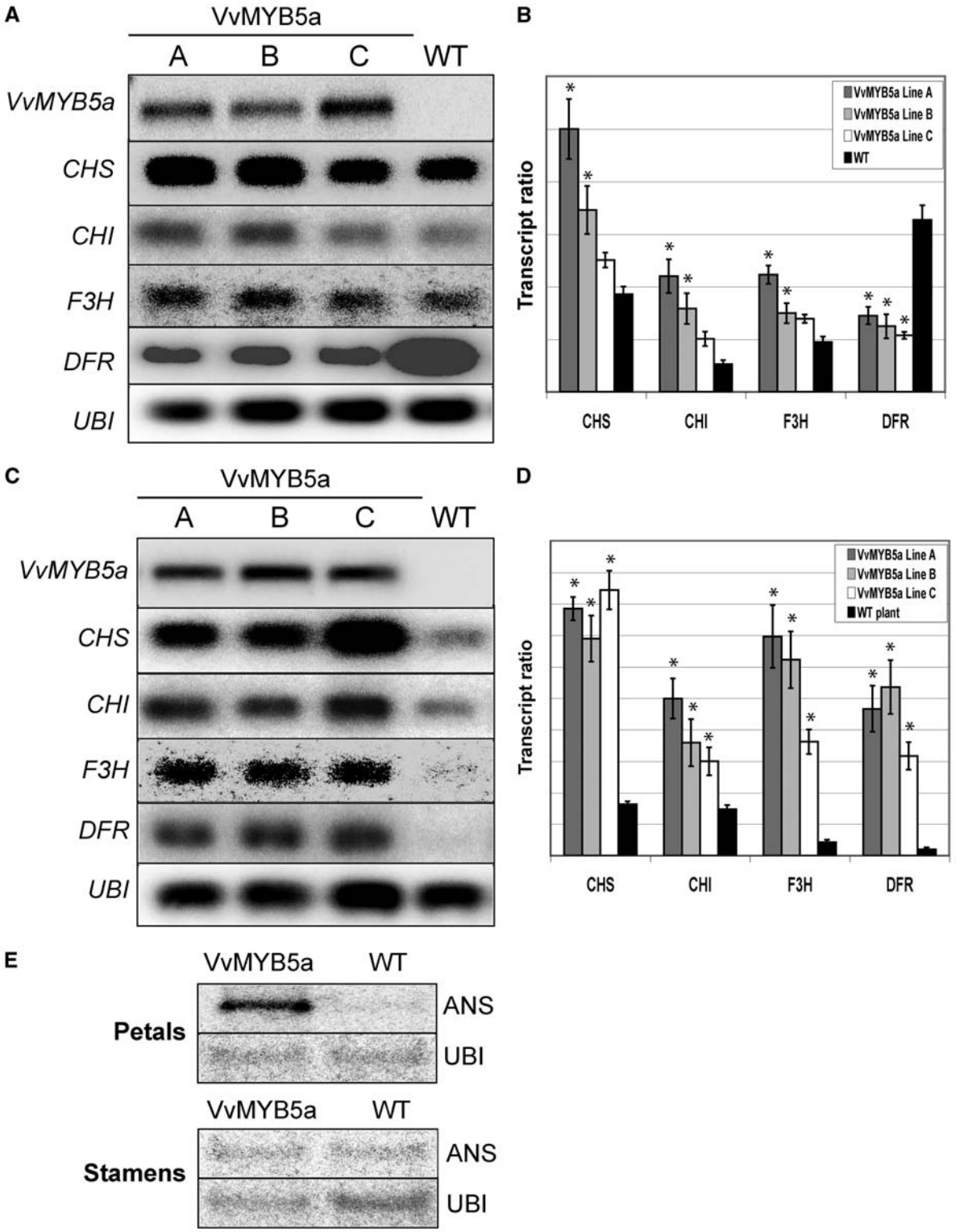

Figure 7. Analysis of transcript accumulation in flowers of transgenic tobacco overexpressing *Vv*MYB5a. A, Transcripts for four flavonoid biosynthetic genes (*CHS*, *CHI*, *F3H*, and *DFR*) were detected by semiquantitative RT-PCR in petals from three *VvMYB5a* independent lines (A–C) and compared to wild-type lines. *VvMYB5a* indicates the transgene expression level. *UBI* was used as a quantitative control. B, Quantification of the RT-PCR results shown in A was performed by measuring the intensity per millimeters squared (Quantity One software; Bio-Rad) of the bands and calculating the ratios between the bands in the gene-specific blot and its corresponding band in the UBI control blot (transcript ratio). Data are means ± SE of two semiquantitative RT-PCR experiments from two independent RNA extractions. Asterisk (*) indicates a significant difference from wild-type plants ($P \leq 0.01$; Student's *t* test). C, Transcripts for four flavonoid biosynthetic genes (*CHS*, *CHI*, *F3H*, and *DFR*) were detected by

structural genes. These transcriptional modifications are accompanied by significant variations of the amounts of phenolic compounds, including anthocyanins, PAs, lignins, and, to a lesser extent, flavonols. In Arabidopsis, ectopic expression of the MYB transcription factor *AtPAP1* leads to the up-regulation of PAL, CHS, and DFR gene expression and is sufficient to enhance production of both lignin and anthocyanin compounds (Borevitz et al., 2000). However, and unlike *PAP1* in Arabidopsis, which appears to be active in the same way in all vegetative and reproductive organs throughout development when overexpressed (Borevitz et al., 2000), the impact of *VvMYB5a* overexpression on the phenylpropanoid pathway in tobacco appears variable, depending on the tissue or organ studied. This difference might provide some interesting information regarding the regulatory mechanisms of the phenylpropanoid pathway in plants. In leaves, overexpression of *VvMYB5a* leads to up-regulation of C4H gene expression, but the genes encoding PAL and 4CL are not affected. In stamens, where no anthocyanins are detected in wild-type plants, *Vv*MYB5a is able to induce transcription of both early and late genes of the anthocyanin pathway, except ANS, and this activation correlates with a strong accumulation of final products in epidermal cells. In petals where anthocyanins are normally synthesized in wild-type plants, overexpression of *VvMYB5a* leads to a moderate activation of structural gene expression and anthocyanins and PAs are produced. Interestingly, DFR gene expression is clearly reduced in transgenic petals, whereas ANS expression increases. In stamens, DFR induction is not correlated with a modification of ANS gene expression. In Arabidopsis, recent work from Abrahams and coworkers (2003) indicates that ANS is not only a key enzyme for the formation of anthocyanins but also is essential for PA synthesis. In the anthocyanin and CT biosynthesis pathway (Fig. 1), a high ANS activity would lead to the accumulation of anthocyanidins, which are subsequently substrates for anthocyanin synthesis via 3-glucosyltransferase (3GT) and/or CT biosynthesis via anthocyanidin reductase (ANR). Because of the competition between 3GT and ANR for substrate, this particular step of the phenylpropanoid pathway may represent the control point between anthocyanin and PA biosynthesis (Dixon et al., 2005). According to our results, it is possible that low anthocyanidin concentrations would favor 3GT activity and the anthocyanin pathway, whereas higher concentrations would allow 3GT and ANR activities and lead to anthocyanin and CT biosynthesis. Whether high ANS gene expression can be related to the decrease in DFR gene expression in transgenic petals remains to be investigated.

Apart from the anthocyanins and PA metabolism, overexpression of *VvMYB5a* also impacts on lignin biosynthesis. In anther cells, lignified fibers were partially missing in transgenic plants, resulting in delayed dehiscence. These observations probably reflect the impact of *VvMYB5a* overexpression in the regulatory mechanisms of the monolignol pathway. The decrease in expression of two *CCoAOMT* genes in transgenic lines is consistent with previous results demonstrating the key role of CCoAOMT for both lignin accumulation and composition in plants (Zhong et al., 1998). Our observations may also be compared with recent findings concerning a *MYB* gene, named *AtMYB26*, which regulates cell wall fortification in endothecium cells (Steiner-Lange et al., 2003). Likewise, failure in anther dehiscence is also observed in *HvGAMYB* sense barley (*Hordeum vulgare*) plants where anther development is altered and results in male sterility (Murray et al., 2003). However, the fact that *AtMYB26* and *HvGAMYB* gene expression occurred exclusively in inflorescences, whereas *VvMYB5a* was expressed in all grapevine tissues, suggests that its regulatory mode and array of target genes could be different.

A Putative Role for *Vv*MYB5a in Grapevine?

While *Vv*MYB5a is able to regulate various branches of the phenylpropanoid pathway when overexpressed in tobacco, the function of this R2R3-MYB regulatory protein remains to be determined in grapevine. However, some lines of evidence indicate that *VvMYB5a* might also be involved in the control of the phenylpropanoid pathway in grapevine. In grape berry skin, a strong expression of genes encoding enzymes of the anthocyanin biosynthetic pathway, except UFGT, is detected up to 4 weeks after flowering. This first activation of gene expression is followed by a regular decrease in transcript abundance up to the véraison stage, where a second activation occurs for all genes, including UFGT, and coincides with the onset of anthocyanin biosynthesis (Boss et al., 1996). Such expression patterns indicate that anthocyanin biosynthesis in berry skin may be under the control of at least two types of regulatory factors, one expressed early during berry development that will induce expression of all structural genes, except UFGT, and another expressed later that will induce expression of all genes, including

Figure 7. (*Continued*.)
semiquantitative RT-PCR in stamens from three *VvMYB5a* independent lines (A–C) and compared to wild-type lines. *VvMYB5a* indicates the transgene expression level. *UBI* was used as a quantitative control. D, Quantification of the RT-PCR results shown in C was performed by measuring the intensity per millimeters squared (Quantity One software; Bio-Rad) of the bands and calculating the ratios between the bands in the gene-specific blot and its corresponding band in the UBI control blot (transcript ratio). Data are means ± SE of two semiquantitative RT-PCR experiments from two independent RNA extractions. Asterisk (*) indicates a significant difference from wild-type plants ($P \leq 0.01$; Student's *t* test). E, Northern-blot analysis of *ANS* gene expression in petals and stamens from wild-type and *VvMYB5a* lines. Total RNA was extracted from tissues harvested at the opening of flowers. Experiments were repeated with three *VvMYB5a* and wild-type lines with similar results.

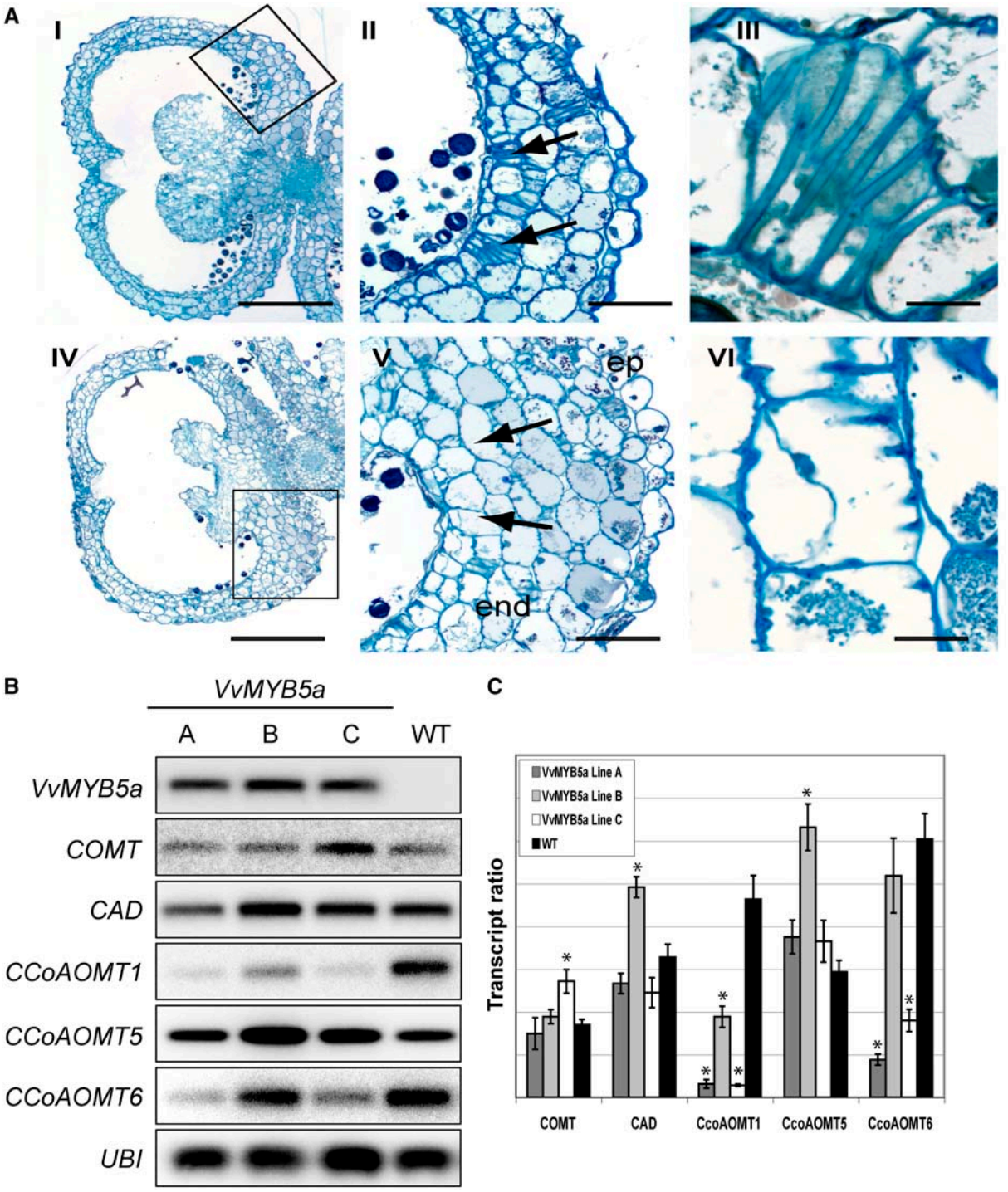

Figure 8. Modification of monolignol metabolism in transgenic anthers. A, Cross sections of anthers at stage 10 from wild-type (I–III) and *VvMYB5a*-overexpressing tobacco plants (IV–VI). Arrows indicate endothecial cells developing complete (II) or incomplete (V) lignified fibers (shown more enlarged in III and VI, respectively). ep, Epidermis; end, endothecium. Bars = 500 μm (I and IV), 100 μm (II and V), and 20 μm (III and VI). B, Transcripts for monolignol biosynthetic genes (*COMT*, *CAD*, and *CCoAOMT1*, *5*, and *6*) were detected by semiquantitative RT-PCR in stamens from three *VvMYB5a* independent lines (A–C) and compared to wild-type lines. *VvMYB5a* indicates the transgene expression level. *UBI* was used as quantitative control. C, Quantification of the RT-PCR results shown in B was performed by measuring the intensity per millimeters squared (Quantity One software; Bio-Rad) of the bands and calculating the ratios between the bands in the gene-specific blot and its corresponding band in the UBI control blot (transcript ratio). Data are means ± SE of two semiquantitative RT-PCR experiments from two independent RNA extractions. Asterisk (*) indicates a significant difference from the wild-type plants ($P \leq 0.01$; Student's *t* test).

Table IV. *Primers for RT-PCR analysis*

Genes	Accession No.	Sense Primers	Antisense Primers
Nt-PAL	D17467	5′-GCCAACAGGATAAAAGAATGC	5′-TCCCACAATATAAGCCCAAGC
Nt-4CL	U50845	5′-CACACTGGCCACATTGGGTTCATT	5′-TTCGCCCGTTGCCAAACTGGAAAT
Nt-CHS	AF311783	5′-CCTTTGGGAATTTCTGATTGG	5′-TCCCACAATATAAGCCCAAGC
Nt-F3H	AF036169	5′-AGCTAGAGACTACTCCAGGTG	5′-AACCGTGATCCAAGTTTTGCCA
Nt-COMT	X74453	5′-CTTGGAGGATTAAGCAATATA	5′-AAGCTTTTTCCTAACACACTGC
Nt-CAD	X62343	5′-ACTGCAATGGAGAGGTTTGGAG	5′-TACATAAACGTCACTCTCGATCAC
Nt-CCoAOMT-1	U38612	5′-AACCGGGAAAACTACGAGATTGGT	5′-TCTTGGTTGCCACAAATGACGAT
Nt-CCoAOMT-5	AF022775	5′-GGGTACTCCCTCCTTGCTACTGCC	5′-ATATTGGAATGATCAGGTGATGCG
Nt-CCoAOMT-6	Z56282	5′-GACAACACCCTATGGAATGG	5′-ATAGCGATAATCATGAGATAC
Nt-UBI	U66264	5′-TCCAGGACAAGGAGGGTAT	5′-GAGACCTCAGTAGACAAAGC
VvMYB5a-3′-UTR	AY555190	5′-CCCCACCCAGCAATTTCTGTG	5′-CCATTTCACATACGATATTCACAC
Vv-EF-γ	AF176496	5′-GCGGGCAAGAGATACCTCAA	5′-TCAATCTGTCTAGGAAAGGAAG

UFGT. Another possibility is the presence of regulatory factors expressed before and after véraison and regulating the expression of all structural genes, except UFGT, along with regulatory factors specifically regulating UFGT gene expression and expressed only after véraison (Boss et al., 1996). The recent characterization of a MYB gene from *V. labruscana* regulating specifically UFGT gene expression (Kobayashi et al., 2002) appears to favor this second possibility. In this case, the high expression of *VvMYB5a* before véraison in all berry tissues studied may indicate its implication in the first activation of structural gene expression observed during the early steps of grape berry development. If so, and, as already suggested by its expression pattern in this organ, *Vv*MYB5a would not be directly involved in the anthocyanin accumulation observed in grape berry skin after véraison. However, the enzymes implicated in this first activation are also necessary for other biosynthetic pathways, notably those leading to flavonols and PAs (Fig. 1). Interestingly, in grape seeds, PAs accumulate mainly between fruit set and véraison (Downey et al., 2003), when *VvMYB5a* is highly expressed. In this tissue, epicatechin is the major constituent representing about 65% of the total PA subunits (Downey et al., 2003). Thus, the strong accumulation of epicatechin-derived compounds in petals of *VvMYB5a*-overexpressing tobacco plants might suggest a role for this regulatory factor in the control of PA biosynthesis in grape seeds.

In any case, further work in a homologous system, like loss-of-function experiments, is now required to determine the precise function of *Vv*MYB5a. Reproducible genetic engineering is slowly becoming a reality in grapevine, but, in our case, loss-of-function experiments may be difficult to interpret because of the possible functional redundancy within the R2R3-MYB family in plants (Jiang et al., 2004). In the case of gene families that have functional redundancy, related family members may have to be suppressed to observe a phenotype (Liljegren et al., 2000). Thus, identification of all the *R2R3-MYB* genes in the grape genome appears to be a prerequisite for undertaking the functional characterization of grapevine MYB genes in a homologous system. Complete sequencing of the grape genome will probably allow such experiments to take place in the coming years and will definitely be useful for ascertaining the role of MYB transcription factors in the regulation of the phenylpropanoid pathway in grapevine.

MATERIALS AND METHODS

Plant Material and Growth Conditions

Berries from grape (*Vitis vinifera*) L. cv Cabernet Sauvignon plants from the Domaine du Grand Parc (Institut National de la Recherche Agonomique) were sampled at 2-week intervals during the 2002 and 2003 growing seasons. Berry development stages were chosen according to criteria including size, measures of soluble sugars, softening, and coloring of the berries as previously described by Boss et al. (1996). Berries for RNA extraction were sampled and immediately frozen in liquid nitrogen before storage at −80°C pending further analysis. Separate skin and flesh samples were obtained by peeling fresh berries just before freezing in liquid nitrogen.

Wild-type and transgenic tobacco (*Nicotiana tabacum* cv Xanthii) seeds were sterilized in 70% ethanol for 2 min followed by 2.5% potassium hypochlorite for 10 min, and finally washed three times with sterile water. After cold treatment at 4°C for 48 h, seeds were germinated in tissue culture conditions at 23°C under a 16-h-light/8-h-dark regime on Murashige and Skoog medium (Murashige and Skoog, 1962) containing 3% (w/w) Suc and 100 μg/mL kanamycin for transgenic plants. Tobacco plants were finally transferred to soil and grown in individual pots in a greenhouse.

Cloning of *Vv*MYB5a cDNA and Plant Transformation

A cDNA library from grape L. cv Cabernet Sauvignon berries (véraison stage) was constructed using the SMART cDNA library construction kit (CLONTECH) and used as a template for PCR cloning. Two degenerated oligonucleotides designed from plant MYB cDNA conserved sequences, 5′-GANRTMAARAAYTAYTGGAACWCN-3′ (forward) and 5′-NGTGTTC-CARTARTTYTTKAYNTC-3′ (reverse) were used in combination with the T7 and 5′ primers located in the pTriplex vector (CLONTECH). PCR products were cloned into the pGEM-T-easy plasmid (Promega) and sequenced on both strands (Genome Express). Specific oligonucleotides defined within the 5′ and 3′ noncoding regions were used to amplify the *Vv*MYB5a full-length cDNA.

For plant transformation, the complete coding sequence of *Vv*MYB5a cDNA was amplified with a specific forward primer designed to introduce a *Xba*I restriction site (5′-AACCAATGGATCCGTCTAGAGAGA-3′) and a reverse primer designed to introduce a *Sac*I restriction site (5′-CAAGAGTGG-GAGCTCATACAACATC-3′). The *Xba*I/*Sac*I fragment was cloned into binary vector pGiBin19 (provided by Dr. D. Inzé, Gent, Belgium) between the 35S promoter of *Cauliflower mosaic virus* and the nopaline synthase poly(A) addition site, creating the pGiBin19-*Vv*MYB5a plasmid. The construction was introduced into *Agrobacterium tumefaciens* LB4401 strain. Leaf disc transformation and regeneration of transgenic plants were performed as previously described (Horsch et al., 1986). Transformed tobacco plants were

selected using kanamycin (100 μg/mL) as a selective marker. Fifteen independent lines from the T_2 progeny of transgenic plants showing no phenotypic variations were used for further analysis and compared to wild-type nontransformed lines grown in the same conditions (Aharoni et al., 2001).

RNA Extraction and Analysis

Three different procedures of RNA extraction were used, depending on the plant material. Total RNAs from grape berry tissues were extracted according to the method described by Asif et al. (2000). RNA from wild-type and transformed tobacco leaves were extracted using RNeasy plant mini kits (Qiagen), according to the manufacturer's instructions. Finally, total RNA from tobacco flower tissues was extracted as described by Verwoerd et al. (1989). All RNA samples were treated with RNase-free DNase I (Promega) followed by phenol-chloroform extraction and ethanol precipitation. No DNA contamination was detected based on PCR amplification. All RNA analyses were performed at least three times with three independent samples. For semiquantitative RT-PCR assays, gene-specific primers were chosen preferentially in the 3′-UTR regions of the target mRNAs and are listed in Table IV. To estimate the transcript levels of the *VvMYB5a* transgene in tobacco, we used a forward primer specific for *VvMYB5a* (5′-CCCCACCCAGCAATTTCTGTG-3′) in combination with a reverse primer designed from the 3′ transcribed region of the nopaline synthase terminator (5′-TCATCGCAAGACCGGCAACA-3′). Specific primers for tobacco CHI, DFR, and C4H were designed from cDNA clones generously provided by Dr. Cathie Martin (John Innes Centre) to whom requests may be addressed. The ANS cDNA probe from petunia (*Petunia hybrida*) was provided by Dr. Asaph Aharoni (Plant Research International). In all cases, cloning and sequencing the RT-PCR products confirmed the amplification specificity.

For RT-PCR analysis, 1 μg of total RNA was reverse transcribed with oligo(dT) 12 to 18 in a 20-μL reaction mixture using the Maloney murine leukemia virus reverse transcriptase (Promega) according to the manufacturer's instructions. After heat inactivation of the reaction mixture, PCR was performed using 1 μL of the first-strand cDNA sample with 25 pmol of the primers shown in Table I in a 50-μL reaction. For all experiments presented in this study, 15 cycles of PCR amplification were performed, except for the detection of the *VvMYB5a* transgene in tobacco, where 20 cycles were performed. RT-PCR products were separated on agarose gels and analyzed by DNA gel-blot hybridization using random-primed ^{32}P gene-specific probes, according to standard protocols (Sambrook et al., 1989). Signals were visualized with an FX molecular imager (Bio-Rad) and quantified using Quantity One software (Bio-Rad). The relative expression level for each target gene was determined by calculating the ratio of the target gene intensity to the *ubiquitin* (UBI) intensity signal obtained from the same cDNA preparation.

RNA gel blots were prepared and hybridized according to standard protocols (Sambrook et al., 1989). Equal loading of RNA samples and uniform transfer onto membranes were confirmed by ethidium bromide staining of the RNA gels and/or hybridization with a ^{32}P-labeled UBI probe. After hybridization at 42°C, membranes were washed at room temperature three times for 20 min each in 1 × SSC and 0.1% SDS, followed by one wash in 0.2 × SSC and 0.1% SDS at 65°C for 15 min before exposure to a phosphor-imager screen (Molecular Imager FX; Bio-Rad).

Quantification of Anthocyanins from Petal and Stamen Extracts

Petal limbs and stamens were harvested from transgenic and wild-type tobacco plants at equivalent ages and submitted to freeze drying. Each sample (30 mg dry weight) was extracted with methanol 0.32 M HCl (85:15, v/v) overnight at 4°C. After centrifugation (3,000 rpm, 5 min), absorbance of the supernatant was measured at 535 nm with a Secoman S250 spectrophotometer. Total anthocyanin content was calculated according to the extinction coefficient (E1% = 461 at this wavelength in the same solvent) of keracyanin (cyanidin-3-rhamnoglucoside) purified from transgenic and wild-type tobacco flowers or purchased from Extrasynthese. Each extract was then diluted with an equal volume of water. One-hundred microliters of each diluted sample were analyzed by HPLC with a Prontosil Eurobound C18 (5 μM) reversed-phase column (4 mm i.d. × 250 mm; Bischoff) with guard column. Solvents used for the separation were 0.1% trifluoroacetic acid in water (A) and 0.1% trifluoroacetic acid in acetonitrile (B). The elution program at 0.6 mL/min was 12% to 26% B (0–35 min), 26% to 100% B (35–36 min), 100% B (36–49 min), 100% to 12% B (49–50 min), and 12% B (50–60 min). The chromatogram was monitored at 521 nm. Keracyanin content was estimated from a calibration curve obtained with pure compound using the same HPLC conditions. HPLC analyses and purification were carried out on a Gilson gradient system equipped with a UV visible detector (Spectra Physics model SP8450). Mass spectra were recorded with VG Autospec-Q in the fast-atom bombardment$^+$ mode. NMR spectra were recorded at 303 K on a 500-MHz Bruker spectrometer using CD_3OD as a solvent. All analyses were performed three times throughout these investigations.

Quantification of PA-Derived Compounds

Extraction of CTs was carried out as described by Geny et al. (2003) and measurements were performed according to the method of Saucier et al. (2001). HPLC analyses were carried out on a Spectra Physics system fitted with a UV visible detector driven by a PC1000 system. Each extract was then diluted 10-fold with methanol and analyzed by HPLC with a HYPERSIL-KEYSTONE R BDS-C18 (5 μM) reversed-phase column (4 mm i.d. × 250 mm). Solvents used for the separation were acetic acid (5%) in water (A) and methanol in acetic acid solution (B). The elution program at 1 mL/min was 30% to 60% B (0–15 min), 100% B (16–25 min), and 30% B (26–30 min).

Histology of Anthers and Histochemical Staining of CTs

For histological studies, anthers from wild-type or transgenic tobacco were successively fixed by 2.5% glutaraldehyde, 1% osmium tetroxide, and 1% tannic acid, dehydrated in ethanol and epoxypropane, and embedded in epon. Semithin sections, 2.5-μm thick, were stained by 0.05% toluidine blue in sodium tetraborate containing water. Lignin-containing cell walls are heavily blue stained.

CTs were visualized according to Porter (1989) by incubating tissue slices in a mixture of ethanol:6 M HCl (1:1, v/v) containing 0.1% (w/v) DMACA (Sigma-Aldrich) for 3 to 6 min, then washing three times with water. The samples were observed with a Zeiss Axiophot microscope and digitized pictures were obtained with a Spot camera (Diagnostic Instruments).

Sequence and Phylogenic Analyses

BLAST (National Center for Biotechnology Information) was used for sequence searches. Sequence analysis was performed using Vector NTI Suite (Invitrogen) and BLAST (Altschul et al., 1990) at the National Center for Biotechnology Information (http://www.ncbi.nlm.nih.gov). Multiple sequence alignments and phylogenic analyses were performed using Vector NTI Suite and Multalin (Corpet, 1988; http://prodes.toulouse.inra.fr/multalin/multalin.html). These two methods gave similar results regarding sequence homologies and phylogenic positioning of *Vv*MYB5a. Tree View software (Page, 1996) was used to optimize the presentation of the phylogenic tree in Figure 2.

The GenBank accession number for the *VvMYB5a* cDNA described in this article is AY555190. Accession numbers for the sequences shown in Figure 2 are as follows: c-MYB (X52125), *Am*Divaricata (AAL78741), *Ph*MYB3 (CAA78388), *At*GL1 (P27900), *Zm*-P (AAB67720), *Zm*P1 (M37153), *Zm*C1 (AAA33482), *Vl*MYBA2 (BAC07540), *At*PAP1 (AAG42001), *Ph*AN2 (AAF66727), *Le*ANT1 (AAQ55181), *Os*MYB4 (T02988), *At*MYB5 (U26935), *Bn*LGHi233 (AF336278), *Vl*MYBB1 (BAC07543), *Ph*MYB1 (Z13996), *Am*Mixta (CAA55725), *At*MYB4 (BAA21619), *Fa*MYB1 (AAK84064), *Am*MYB330 (JQ0957), and *Am*MYB308 (JQ0960). Accession numbers for the regions used as gene-specific probes are listed in Table IV.

ACKNOWLEDGMENTS

We thank Pr. Dr. Serge Delrot and Dr. Christopher Augur for comments and advice on the manuscript and Dr. L. Geny for PA analysis and quantification. We are grateful to Dr. Cathie Martin and Dr. Asaph Aharoni for providing some of the cDNA probes used in this study.

Received June 17, 2005; revised December 6, 2005; accepted December 6, 2005; published December 29, 2005.

LITERATURE CITED

Abrahams S, Lee E, Walker AR, Tanner GJ, Larkin PJ, Ahston AR (2003) The *Arabidopsis TDS4* gene encodes leucoanthocyanidin dioxygenase (LDOX) and is essential for proanthocyanidin synthesis and vacuole development. Plant J **35:** 624–636

Aharoni A, Ric de Vos HC, Wein M, Sun Z, Greco R, Kroon A, Mol JNM, O'Connell AP (2001) The strawberry *FaMYB1* transcription factor

suppresses anthocyanin and flavonol accumulation in transgenic tobacco. Plant J **28:** 319–322

Altschul SF, Gish W, Miller W, Myers EW, Lipman DJ (1990) Basic local alignment search tool. J Mol Biol **215:** 403–410

Asif MH, Dhawan P, Nath P (2000) A simple procedure for the isolation of high quality RNA from ripening banana fruit. Plant Mol Biol Rep **18:** 105–119

Bagchi D, Bagchi M, Stohs SJ, Das DK, Ray SD, Kuszynski CA, Joshi SS, Pruess HG (2000) Free radicals and grape seed proanthocyanidin extract: importance in human health and disease prevention. Toxicology **148:** 187–197

Bagchi D, Sen CK, Ray SD, Das DK, Bagchi M, Preuss HG, Vinson JA (2003) Molecular mechanisms of cardioprotection by a novel grape seed proanthocyanidin extract. Mutat Res **523-524:** 87–97

Borevitz JO, Xia Y, Blount J, Dixon RA, Lamb C (2000) Activation tagging identifies a conserved MYB regulator of phenylpropanoid biosynthesis. Plant Cell **12:** 2383–2394

Boss PK, Davies C, Robinson SP (1996) Analysis of the expression of anthocyanin pathway genes in developing *Vitis vinifera.* Plant Physiol **111:** 1059–1066

Cone KC, Burr FA, Burr B (1986) Molecular analysis of the maize anthocyanin regulatory locus *C1.* Proc Natl Acad Sci USA **83:** 9631–9635

Corpet F (1988) Multiple sequence alignment with hierarchical clustering. Nucleic Acids Res **16:** 10881–10890

Dixon RA, Xie DY, Sharma SB (2005) Proanthocyanindins—a final frontier in flavonoid research? New Phytol **165:** 9–28

Downey MO, Harvey JS, Robinson SP (2003) Analysis of tannins in seeds and skins of Shiraz grapes throughout berry development. Aust J Grape Wine Res **9:** 15–27

Fauconneau B, Waffo Teguo P, Huguet F, Barrier L, Decendit A, Mérillon JM (1997) Comparative study of radical scavenger and antioxidant properties of phenolic compounds from *Vitis vinifera* cell cultures using in vitro tests. Life Sci **61:** 2103–2110

Geny L, Saucier C, Bracco S, Daviaud F, Glories Y (2003) Composition and cellular localization of tannins in grape seeds during maturation. J Agric Food Chem **51:** 8051–8054

Glories Y (1988) Anthocyanins and tannins from wine: organoleptic properties. *In* V Cody, ed, Plant Flavonoids in Biology and Medicine II: Biochemical, Cellular, and Medicinal Properties. Alan R. Liss, New York, pp 124–134

Grotewold E, Sainz MB, Tagliani L, Hernandez JM, Bowen B, Chandler VL (2000) Identification of the residues in the MYB domain of maize C1 that specify the interaction with the bHLH cofactor R. Proc Natl Acad Sci USA **97:** 13579–13584

Hollman PC, Katan MB (1999) Dietary flavonoids: intake, health effects and bioavailability. Food Chem Toxicol **37:** 937–942

Holton TA, Cornish EC (1995) Genetics and biochemistry of anthocyanin biosynthesis. Plant Cell **7:** 1071–1083

Horsch RB, Klee HJ, Stachel S, Winans SC, Nester EW, Rogers SG, Fraley RT (1986) Analysis of *Agrobacterium tumefaciens* virulence mutants in leaf discs. Proc Natl Acad Sci USA **83:** 2571–2575

Jiang C, Gu X, Peterson T (2004) Identification of conserved gene structures and carboxy-terminal motifs in the Myb gene family of Arabidopsis and Oryza sativa L. ssp. Indica. Genome Biol **5:** R46

Jin H, Cominelli E, Bailey P, Parr A, Mehrtens F, Jones J, Tonelli C, Weisshaar B, Martin C (2000) Transcriptional repression by *AtMYB4* controls production of UV-protecting sunscreens in Arabidopsis. EMBO J **19:** 6150–6161

Kennedy JA, Troup GJ, Pilbrow JR, Hutton DR, Hewitt D, Hunter CR, Ristic R, Iland PG, Jones GP (2000) Development of seed polyphenols in berries from *Vitis Vinifera* L. cv. Shiraz. Aust J Grape Wine Res **6:** 244–254

Klatsky AL (2002) Alcohol and cardiovascular diseases: a historical overview. Ann NY Acad Sci **957:** 7–15

Kobayashi S, Goto-Yamamoto N, Hirochika H (2004) Retrotransposon-induced mutations in grape skin color. Science **304:** 982

Kobayashi S, Ishimaru M, Hiraoka K, Honda C (2002) MYB-related genes of the Kyoho grape (*Vitis labruscana*) regulate anthocyanin biosynthesis. Planta **215:** 924–933

Koltunow AM, Truettner J, Cox KH, Wallroth M, Golberg RB (1990) Different temporal and spatial gene expression patterns occur during anther development. Plant Cell **2:** 1201–1224

Kranz HD, Denekamp M, Greco R, Jin H, Leyva A, Meissneir RC, Petroni K, Urzainqui A, Bevan M, Martin C, et al (1998) Towards functional characterization of the members of the R2R3-MYB gene family from *Arabidopsis thaliana.* Plant J **16:** 263–276

Lairon D, Amiot MJ (1999) Flavonoids in food and natural antioxidants in wine. Curr Opin Lipidol **10:** 23–28

Li SF, Santini JM, Nicolaou O, Parish RW (1996) A novel MYB related gene from *Arabidopsis thaliana.* FEBS Lett **379:** 117–121

Liljegren SJ, Ditta GS, Eshed Y, Savidge B, Bowman JL, Yanofsky MF (2000) Shatterproof MADS-box genes control seed dispersal in *Arabidopsis.* Nature **404:** 766–770

Lin LC, Kuo YC, Chou CJ (2002) Immunomodulatory proanthocyanidins from *Ecdysanthera utilis.* J Nat Prod **65:** 505–508

Martin C, Prescott A, MacKay S, Bartlett J, Vrijlandt E (1991) The control of anthocyanin biosynthesis in flowers of *Antirrhinum majus.* Plant J **1:** 37–49

Mathews H, Clendennen SK, Caldwell CG, Liu XL, Connors K, Matheis N, Shuster DK, Menasco DJ, Wagoner W, Lightner J, et al (2003) Activation tagging in tomato identifies a transcriptional regulator of anthocyanin biosynthesis, modification and transport. Plant Cell **15:** 1689–1703

Mérillon JM, Huguet F, Fauconneau B, Waffo Teguo P, Barrier L, Vercauteren J, Huguet F (1997) Antioxidant activity of stilbene astringin, newly extracted from *Vitis vinifera* cell cultures. Clin Chem **43:** 1092–1093

Mol J, Grotewold E, Koes R (1998) How genes paint flowers and seeds? Trends Plant Sci **3:** 212–217

Murashige T, Skoog F (1962) A revised medium for rapid growth and bioassays with tobacco tissue culture. Physiol Plant **15:** 473–477

Murray F, Kalla R, Jacobsen J, Gubler F (2003) A role for *HvGAMYB* in anther development. Plant J **33:** 481–491

Page RDM (1996) TREEVIEW: an application to display phylogenetic trees on personal computers. Comput Appl Biosci **12:** 357–358

Paz-Ares J, Ghosal D, Wienand U, Peterson PA, Saedler H (1987) The regulatory *c1* locus of *Zea mays* encodes a protein with homology to MYB proto-oncogene products and with structural similarities to transcriptional activators. EMBO J **6:** 3553–3558

Pervaiz S (2003) Resveratrol: from grapevines to mammalian biology. FASEB J **17:** 1975–1985

Porter LJ (1989) Tannins. *In* JB Harbourne, ed, Methods in Plant Biochemistry. Plant Phenolics, Vol 1. Academic Press, London, pp 389–419

Quattrochio F, Wing JF, Leppen HTC, Mol JNM, Koes RE (1993) Regulatory genes controlling anthocyanin pigmentation are functionally conserved among plant species and have distinct sets of target genes. Plant Cell **5:** 1497–1512

Sambrook J, Fritsch EF, Maniatis T (1989) Molecular Cloning: A Laboratory Manual, Ed 2. Cold Spring Harbor Laboratory Press, Cold Spring Harbor, NY

Saucier C, Mirabel M, Daviaud F, Longieras A, Glories Y (2001) Rapid fractionation of grape seed proanthocyanidins. J Agric Food Chem **49:** 5732–5735

Solano R, Nieto C, Avila J, Cañas L, Diaz I, Paz-Ares J (1995) Dual DNA binding specificity of a petal epidermis-specific MYB transcription factor (*MYB.Ph3*) from *Petunia hybrida.* EMBO J **14:** 1773–1784

Steiner-Lange S, Unte US, Eckstein L, Yang C, Wilson ZA, Schmelzer E, Dekker K, Saedler H (2003) Disruption of *Arabidopsis thaliana MYB26* results in male sterility due to non-dehiscent anthers. Plant J **34:** 519–528

Stracke R, Werber M, Weisshaar B (2001) The R2R3-MYB gene family in *Arabidopsis thaliana.* Curr Opin Plant Biol **4:** 447–456

Torskangerpoll K, Fossen T, Andersen OM (1999) Anthocyanin pigments of tulips. Phytochemistry **52:** 1687–1692

Vannini C, Locatelli F, Bracale M, Magnani E, Marsoni M, Osnato M, Mattana M, Baldoni E, Coraggio I (2004) Overexpression of the rice *OsMYB4* gene increases chilling and freezing tolerance of *Arabidopsis thaliana* plants. Plant J **37:** 115–127

Verwoerd TC, Dekker BMM, Hoekema A (1989) A small scale procedure for the rapid isolation of plant RNAs. Nucleic Acids Res **17:** 2362

Winkel-Shirley B (2002) Biosynthesis of flavonoids and effects of stress. Curr Opin Plant Biol **5:** 218–223

Xie DY, Sharma SB, Paiva NL, Ferreira D, Dixon RA (2003) Role of anthocyanidin reductase, encoded by *BANYULS* in plants flavonoid biosynthesis. Science **299:** 396–399

Zhong R, Morrison WH III, Negrel J, Ye ZH (1998) Dual methylation pathways in lignin biosynthesis. Plant Cell **10:** 2033–2046